UCRL-83559
PREPRINT

COMPUTER DESIGN OF A HIGH EXPLOSIVE VELOCITY AUGMENTED KINETIC ENERGY PENETRATOR

D. B. Tuft
M. J. Murphy

This Paper was Prepared for Submittal to
the Symposium on Computational Methods in
Nonlinear Structural and Solid Mechanics

Washington, D.C.
October 6-8, 1980

April 25, 1980

COMPUTER DESIGN OF A HIGH EXPLOSIVE VELOCITY AUGMENTED KINETIC ENERGY PENETRATOR

D. B. Tuft and M. J. Murphy
University of California
Lawrence Livermore Laboratory
Livermore, California 94550

ABSTRACT

The results of a combined analytical experimental design of a high-explosive velocity augmented kinetic energy penetrator are presented. The objective of the analysis is the design of a velocity augmentor and main charge case. The augmentor design must conform to restrictive volume constraints and provide maximum impulse to the main charge which, in turn, must survive the augmentor loading and penetrate the target.

An explicit finite element hydrodynamic computer code, DYNA2D, employing arbitrary zoning, two-way sliding with gaps, and high explosive equation-of-state is employed as the analytical tool. High strain rate material models are used and predictions are compared to experimental deformations. Shock wave interactions in the main charge case are analyzed and a combination of shock attenuation and wave trapping is employed to reduce loads below failure limits.

The final design provides maximum velocity augmentation while staying within volume constraints and maintaining main charge case integrity. Computed deformations and velocities are experimentally verified. This design analysis method using state-of-the-art code and computer capabilities is shown to be an effective method of simplifying the design process as well as providing necessary design optimization data not previously available.

COMPUTER DESIGN OF A HIGH EXPLOSIVE VELOCITY AUGMENTED KINETIC ENERGY PENETRATOR

D. B. Tuft and M. J. Murphy
University of California
Lawrence Livermore Laboratory
Livermore, California 94550

INTRODUCTION

This paper presents the combined analytical/experimental design of a high explosive velocity augmented kinetic energy penetrator being developed at the Lawrence Livermore Laboratory. A Lagrangian hydrodynamic finite-element computer analysis was combined with high explosive testing to develop the penetrator assembly, which consists of a main charge (MC) and a velocity augmentor (VA) as shown in Fig. 1. At target impact the velocity augmentor detonates increasing the main charge velocity allowing it to penetrate the target and come to rest at the desired depth.

OBJECTIVE

The overall objective of this analysis is the design of the velocity augmentor and main charge case within restrictive volume constraints. This objective has two parts:

(1) Design a velocity augmentor to provide maximum impulse to the main charge within the volume available.

(2) Design a main charge case that will survive the augmentor impulse while delivering the maximum payload to the target.

In order to meet these objectives a combined analytical/experimental

program was developed. The approach used to solve this problem applied the unique resources of the Lawrence Livermore Laboratory which combines an extensive scientific computing capability with a conveniently located explosives test facility.

APPROACH

The approach used to solve this problem was a combined analytical/experimental program that was subdivided into four distinct tasks. An objective was met in each task before going on to the next. The following describes these objectives:

1. Computer Model Development. Select an appropriate analytical code and computer. Generate a finite element mesh and mathematically characterize material properties.
2. Computer Model Calibration. Validate the computer model by correlating analytical predictions to experimental results.
3. MC and VA Design Optimization. Optimize the VA and design the MC case to withstand the VA impulse.
4. Final Experimental Verification. Experimentally confirm the computer predictions.

COMPUTER MODEL DEVELOPMENT

The computer code selected for the analysis, DYNA2D, was developed at LLL by J. O. Hallquist [1]. DYNA2D is an explicit, two-dimensional, plane strain and axisymmetric, Lagrangian hydrodynamic finite-element code. Particular features distinguish DYNA2D from codes previously available for hydrodynamic modeling. First, DYNA2D allows gaps and arbitrary two-way sliding between adjacent materials. This improves the modeling of complex geometries with intersecting material interfaces. Specialization of a contact-impact algorithm allows such interfaces to be

rigidly tied allowing variable zoning without the need for transition regions. Because less simplification or compromise is required in the model, more accurate predictions are possible. Another feature of DYNA2D is its use of quadrilateral finite element zones. These allow arbitrary zoning in which logically regular meshes are not required. Finite elements offer an alternative meshing scheme that for certain geometric configurations can result in reduced mesh entanglement. Moreover, the quadrilateral zones afford an added degree of freedom and are less stiff than triangular zones used in some finite element codes. The third feature is the large number of material models incorporated into the code. Four of the thirteen available material models in DYNA2D were used in this analysis. The four material models are described briefly below:

1. Elastic/Plastic/Hydrodynamic

The shear modulus (G), yield strength (S_y), and hardening modulus (E_t) are required to define the standard engineering properties. An equation of state defines the pressure, P, as

$$P = C_\phi + C_1\mu + C_2\mu^2 + C_3\mu^3 + (C_4 + C_5 + C_6\mu^2)\, E_i$$

where

μ = $\frac{\rho}{\rho_o} - 1$

$\frac{\rho}{\rho_o}$ = ratio of current density to initial density

E_i = internal energy

2. Steinberg/Guinan High Strain Rate Model

The Steinberg/Guinan model is an advanced plasticity model that accounts for thermal softening and strain hardening. It assumes that the

elastic shear modulus and the yield strength of an isotropic material depend upon pressure and internal energy [2]. The yield strength is also governed by effective plastic strain that controls strain hardening. The model is rate-independent and was formulated for use at strain rates greater than 10^5 S^{-1}. In this domain it is assumed that strain rate enhancement has saturated and is no longer a variable affecting yield strength.

The expected flow curve for a typical material subjected to high strain rate explosive loading is shown in Fig. 2. When strain hardening alone is the dominant effect, the curve begins at Y_0 and strain hardens to Y_{max}. The value of Y_{max} is the maximum yield strength to be attained from cold work of the material. The dotted curve in Fig. 2 shows the effect of pressure and temperature on the flow curve. During the early stages of deformation when HE pressure is high, the pressure dominates and raises the yield strength. Later in the process when the HE pressure is no longer dominant, the effects of heating due to a rise in internal energy begin to degrade the strength of the material.

3. Jones/Wilkins/Lee High Explosive Equation of State [3]

The JWL equation of state defines the pressure, P, as

$$P = A\left(1 - \frac{\omega}{R_1 V}\right) e^{-R_1 V} + B\left(1 - \frac{\omega}{R_2 V}\right) e^{-R_2 V} + \frac{\omega E_i}{V}$$

where A, B, R_1, R_2, and ω are empirical constants, V is the relative volume, and E_i is the internal energy. A programmed burn model based on detonation velocity is used to define detonation times for each explosive zone.

4. Reactive Material Equation of State

The fourth material model used in the analysis was the reactive

material model. This model characterizes a high explosive material acting as a structural member. However, if the energy input into any zone exceeds a minimum energy in the form of the integral of p^2t, the material in that zone detonates using a modified form of the JWL equation of state.

The post processor used for the analysis, THOR, was also developed at LLL by J. O. Hallquist [4]. THOR reads the binary plot files generated by DYNA2D and plots contours, time histories, and deformed shapes. It can compute a variety of strain measures at either Gauss integration or nodal points, interface pressure along slidelines, forces along constrained boundaries, response spectra, and momentum.

This analysis was run on the Cray-I computer, the most advanced scientific computer currently available in the world. DYNA2D coding was vectorized to take advantage of the computor's speed capabilities. This reduced the computing time (and cost) by a factor of seven over the equivalent time of a CDC 7600.

The computational mesh used in the preliminary analysis is presented in Fig. 3a. The finite-element mesh generator, ZONE, developed at LLL by M. J. Burger [5], was used to develop this mesh. The mesh utilizes 1033 nodes, 838 quadrilateral elements, 5 materials, and 7 slide lines located at material interfaces.

The models used for the materials shown in Fig. 3a were as follows:

4330 V Mod Steel	-- elastic/plastic/hydrodynamic
Titanium	-- elastic/plastic/hydrodynamic
Copper	-- Steinberg/Guinan high strain rate
VA Explosive	-- JWL high explosive equation of state
MC Explosive	-- Reactive material model

The constants used for the titanium, copper, and VA explosive were found

in the literature [2, 3, 6]. However, the properties of the steel case and main charge explosive needed additional consideration in order to accurately correlate computer predictions to experimental data.

Static stress-strain data and split Hopkinson bar test data were obtained for the MC explosive [7]. This data showed that the static yield strength of (.000217) Mbar increased to (.000374) Mbar at a strain rate of 2500 sec^{-1}. The bulk modulus of.10355 Mbar was obtained from ultrasonic tests [8].

High strain rate split Hopkinson bar tests were also run on the 4330 vanadium modified steel case [7]. Strain rates up to 10^3 sec^{-1} are obtainable with the test apparatus at LLL. However, rates as high as 10^5 sec^{-1} can be expected for HE interaction problems. To account for the effect of higher strain rates, the tangent modulus in the elastic/plastic/hydrodynamic material model was held constant while the yield strength was increased until correlation to experimental data was achieved.

CODE CALIBRATION AND EXPERIMENTAL RESULTS

The objective of this portion of the design/analysis was to calibrate and/or validate computer predictions of a non-optimized experimental configuration and to determine acceptable limits of case strain. The initial computer runs were made using three yield strength models. Fig. 3b presents various computed deformations for S_y = 0.0113, 0.0136, and 0.0170 Mbar. Also shown are the corresponding experimental deformations from two tests. The predictions of radial deformation (ΔA), base deformation (B) an overall length change (ΔC) were compared to the results of two explosive experiments. Excellent correlation was found using the yield strength at 0.0170 Mbar which corresponds to a 51% increase over the quasi-static value. Figs. 3c and 3d show a comparison

of the experimental and computed deformed (S_y = .0170 Mbar) geometries.

Further code verification was accomplished by comparing the computed to experimental MC rigid-body velocity from detonation of the velocity augmentor. The experimental velocity was determined using a flash x-ray system. The computed value of 95 M/sec compared well with the experimental value of 92.6 M/sec. The case deformation of 16% was also used as a limit for further designs since the MC survived the augmentor detonation. Although laboratory tests have shown up to 20% strain for this material at static rates, it was decided that 16% deformation should be used for analytical design purposes. A secondary factor in this consideration was the increased cross-sectional area of the MC at the higher deformation levels which reduces penetration.

Although this preliminary velocity augmentor design did not meet volumetric constraints, the analysis and experiment met the objectives of the first two tasks outlined in the program. The following summarizes the results of the first half of the development of the kinetic energy penetrator assembly.

(1) Analytical code calibrated and verified.

(2) Material models defined and confirmed with experimental results.

(3) Deformation limits defined.

VELOCITY AUGMENTOR OPTIMIZATION

The next step was optimization of the velocity augmentor within the imposed volume constraints. Variables chosen for this optimization study were tamping thickness, tamping materials, and shock wave attenuator thickness. These parameters were identified as having a major impact on performance and each was isolated and studied. Maximum MC case velocity

and the experimentally determined limit of 16% radial case strain were used as performance criteria. Designs not meeting augmentor volume and case deformation constraints were not considered.

Because case survivability is a necessity, the velocity augmentor should be designed to do as little damage as possible while producing the highest possible velocity. One of the parameters affecting case damage is shock waves propagating from the augmentor. To reduce the effect of these shock waves on the MC case, a shock attenuator is required. The attenuator material should have high strength, be as light as possible, and have a shock impedence mismatch with the steel case. Titanium was initially chosen as the attenuator material due to its weight, strength, and shock impedence properties. At this point in the design analysis, the thickness of titanium attenuator was set at .953 cm because this proved acceptable in the preliminary design.

H.E. TAMPING OPTIMIZATION

The next parameter to be studied in the velocity augmentor design was the explosive tamper. With the above defined attenuator, tamping was added first in equal radial and longitudinal increments and later in unequal increments. Throughout the tamping optimization, the attenuator thickness and overall outside VA envelope was held constant. This results in a trade off between H.E. mass and tamper mass. Fig. 4a shows MC calculated rigid-body velocity and Fig. 4b shows calculated maximum radial case strain plotted versus augmentor charge-to-mass ratio. From this figure it can be seen that both MC velocity and strain reach a maximum at a charge to mass ratio of .17. This configuration was considered to be optimal. Additional points at higher and lower tamper densities were also calculated.

The resulting optimized velocity augmentor design, shown in Fig. 5,

consists of radially and axially tamped high explosive and a titanium shock attenuator. During the velocity augmentor optimization process, shock wave attenuation was not optimized and case stress levels were not considered. An experimental test of the optimized VA design produced catastrophic MC case failure. Although the calculated maximum radial case deformation for this design was below the acceptable level, the tensile stress in the case far exceeded the tensile strength of the case material. A study of the H.E. shock wave interaction at the MC base showed a compression wave reflecting off the outer case diameter was responsible for the tensile stress failure in the case. Fig. 6 illustrates the sequence of shock interactions leading to high tensile stresses. The spherical wave created by the H.E. detonation enters the base center beginning at about 2μs. The wave then propagates striking the upper side of the case base at about 6μs and reflecting as a tensile wave as shown in Fig. 6c. The initial wave continues to propogate radially outward impacting the outer case wall and reflecting as a strong tensile wave beginning at about 10μs. The stress level of the reflected wave grows in magnitude until reaching a maximum of about 66 Kbar at 12μs, as shown in Fig. 6f. The location of failure in the tested MC case corresponds to the location of this calculated maximum stress.

Two approaches toward reducing tensile stress in the case were taken. First, the magnitude of the compression wave impacting the outer wall was reduced by optimizing the shock wave attenuator. Second, a radial momentum trap was incorporated to absorb the compressive wave at the outer diameter and not allow the reflected tensile wave to propagate back into the case.

SHOCK ATTENUATOR OPTIMIZATION

The shock attenuator, located between the augmentor explosive and the MC case, is intended to reduce shock loading produced by the explosive while at the same time allowing maximum impulse to be imparted to the MC. From one-dimensional shock theory we know that alternating materials of high and low shock impedence will result in minimum stress transmitted.

To evaluate the relative effectiveness of different material combinations and layer thicknesses, several hydrodynamic calculations were performed with KOVEC, a one-dimensional code [9]. KOVEC solves the Lagrangian finite-difference equations for one-dimensional elastic-plastic flow and allows explosive burn using the JWL equation-of-state [3].

The overall geometry for this study is shown at the top of Fig. 7a. The total augmentor length was kept constant to reflect VA volume constraints while the attenuator materials and thicknesses were varied. Hence, explosive thickness varied with changes in attenuator thickness. The MC case was represented by a steel plate with the same thickness as the bottom center thickness of the MC case.

The parameters of interest in this attenuator study were total impulse delivered to the case and maximum pressure in the case. As a baseline, a calculation of impulse for zero attenuation was made and all subsequent impulse numbers were expressed as a fraction of the baseline impulse I_o.

Fig. 7a shows a plot of impulse ratio I/I_o, pressure transmission ratio P_t/P_i, and maximum case pressure as a function of plate thickness for the tantalum-lucite combination. This material combination represents one of the highest possible difference in shock impedence available in common materials. The rise in case pressure between 0.0 and

.159 cm plate thickness is due to pressure magnification differences between a shock impinging on steel or tantalum. Thus, in this instance, two thin attenuator plates are worse than no attenuation at all. The pressure ratio decreases more rapidly than the impulse ratio for plate thicknesses beyond .318 cm. This thickness was selected as an optimum configuration.

Several other material and thickness combinations were also considered. The results indicated the optimum attenuator among those investigated is a .318 cm tantalum - .318 cm lucite combination. This attenuator produced the maximum relative impulse while reducing case pressure below the calculated acceptable level.

Fig. 7b shows a comparison of a two-dimensional calculation of pressure versus time in the bottom center of the MC case for the titanium attenuator and tantalum-lucite attenuator. The maximum pressure has been reduced by 44% and the pulse spread out producing a longer duration, less severe push on the MC case.

MOMENTUM TRAP DESIGN

With the magnitude of the incident stress reduced, it was then desirable to prevent the compression wave from reflecting as a tensile wave at the outer diameter of the case. The momentum trap design shown in Fig. 8 was incorporated to achieve this effect. The momentum trap, which is actually a combination of a third attenuator plate and a radial momentum ring, is made of the MC case steel so that the initial compression wave will pass from the case into the ring with zero reflection. This initial compression wave then reflects from the outer surface of the ring as a tensile wave which cannot propogate through the material interface back into the case. Thus, the tensile wave is trapped

and damage is limited to the ring. Calculations showed the momentum trap design completely eliminated any tensile stress in the case resulting from radial wave reflection. By improving the shock attenuation and preventing radial wave reflection, the maximum tensile stress in the case was reduced from about 66 Kbar to below 20 Kbar. Computed stress from our preliminary experiments suggested that 20 Kbar was an acceptable level for dynamic stress and that the MC case should survive with the new velocity augmentor design.

The new design was tested twice and case integrity was achieved in both experiments. A comparison of calculated to actual deformed geometry of the MC case is shown in Fig. 9. The predicted length, base, and radial deformations are within 13% of the experimental deformations. At this point all of the objectives were met. The augmentor provided sufficient impulse to the main charge while staying within the volumetric constraints. In addition, the main charge survived the impulse and penetrated the target.

CONCLUSIONS

The results of this study indicate that the finite-element calculational method employing arbitrary geometry, two-way slide lines, and H.E. equation-of-state is a valid method for predicting the mechanics of the H.E. detonation phenomena and resulting shock wave interactions. A high-explosive augmented kinetic energy penetrator was designed using this tool and the results were experimentally verified. Maximum velocity augmentation was obtained while staying within VA volume constraints and maintaining MC case integrity. This method can be used to accelerate and simplify the design process as well as provide necessary data for design optimization not previously available.

FUTURE EFFORT

At the present time a baseline for a velocity augmented kinetic energy penetrator assembly has been designed. Feasibility of using a high explosive augmentor within the volumetric and weight constraints has been shown. Our future effort is concerned with optimizing key parameters affecting the overall performance. The following areas of study are planned:

1. Optimize Momentum Trap - The current momentum trap design eliminated undesirable tensile stresses in the case. However, a large portion of the augmentor energy was absorbed in this process. Future effort is directed toward minimizing the absorbed energy while maintaining the current stress levels in the case.
2. Improve overall charge/mass ratio - Effort will continue to reduce case weight and increase the amount of MC explosive.

ACKNOWLEDGMENTS

The authors wish to acknowledge Dr. J. O. Hallquist, Mr. R. E. Varosh and Dr. R. W. Werne for their technical contributions to this work. Our appreciation also goes to Ms. Toni Dry who typed the manuscript.

Work performed under the auspices of the U. S. Department of Energy by the Lawrence Livermore Laboratory under contract number W-7405-ENG-48.

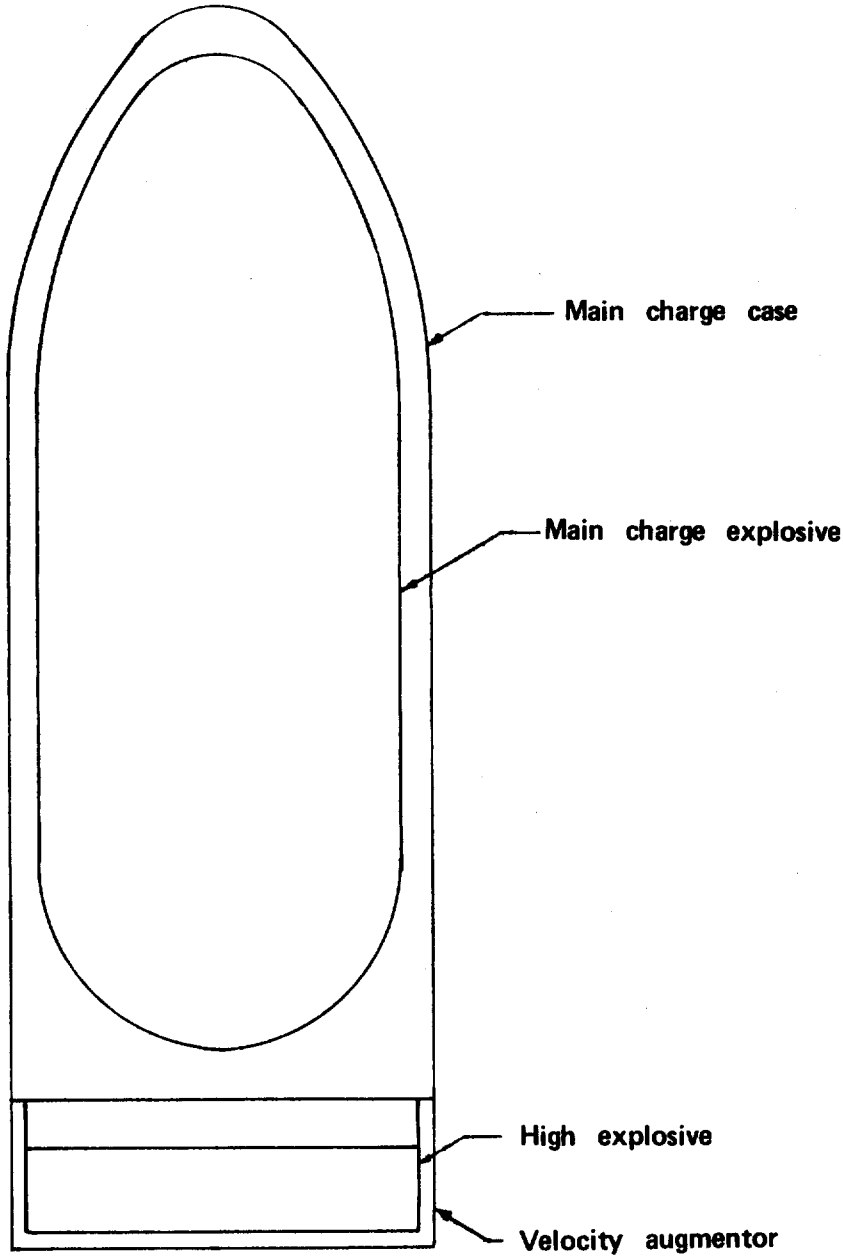

Fig. 1. Kinetic Energy Penetrator Assembly

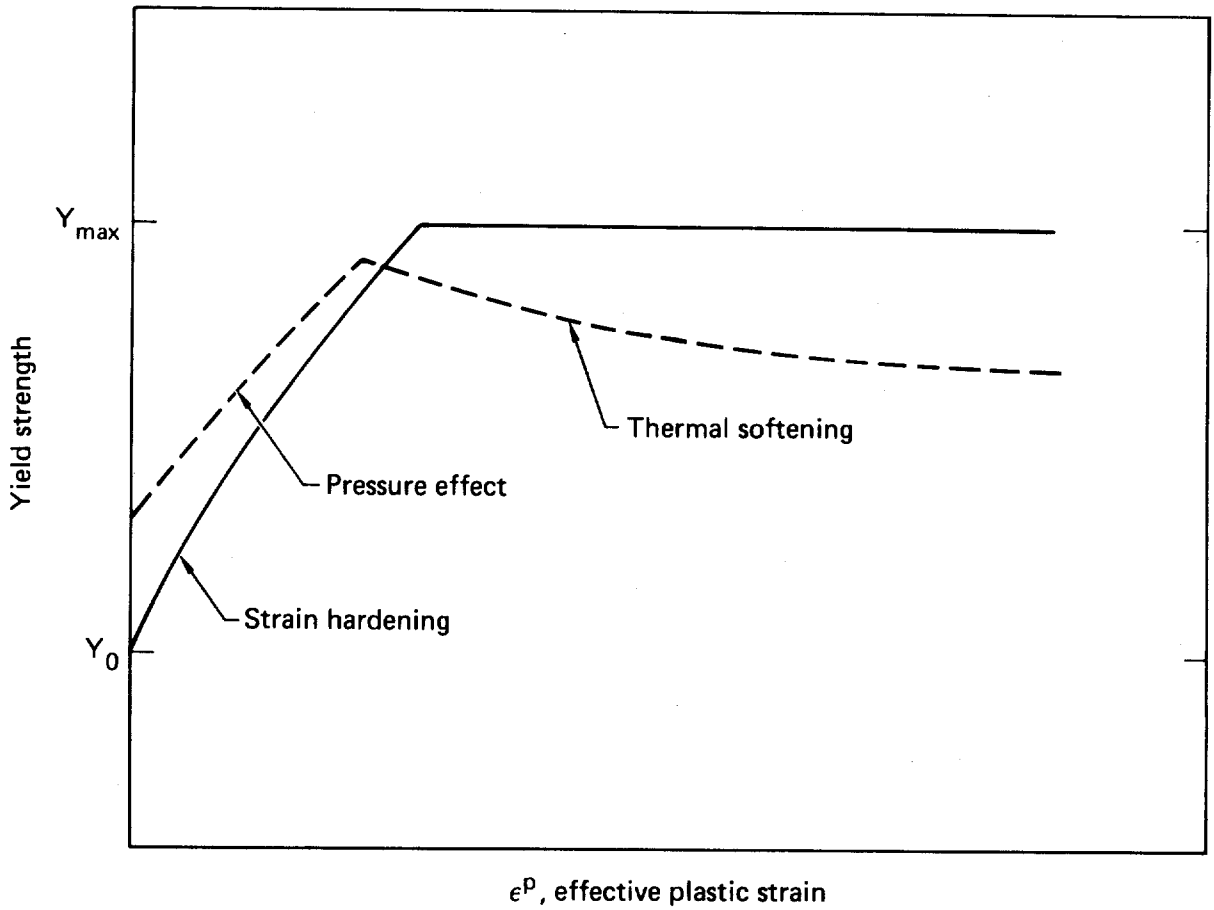

Fig. 2. Steinberg-Guinan High Strain Rate Model

(a)

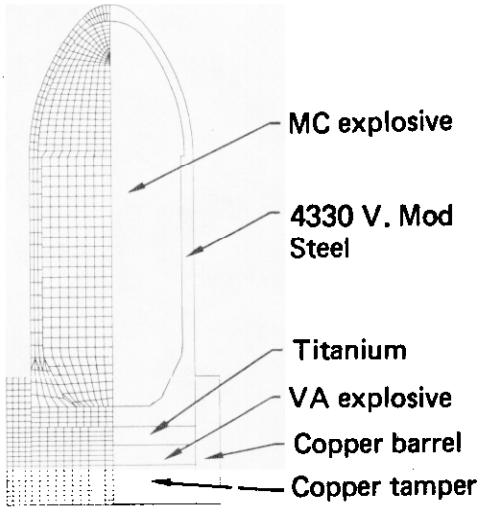

(b)

	YIELD STRENGTH (Mbar)	DEFORMATION (cm)		
		ΔA	B	ΔC
RUN 1	0.0113	1.88	1.40	1.28
RUN 2	0.0136	1.66	1.20	1.10
RUN 3	0.0170	1.30	1.02	0.840
GUN 1	TEST	1.32	1.03	0.838
GUN 2	TEST	1.31	1.03	0.836

(c)

Experiment

(d)

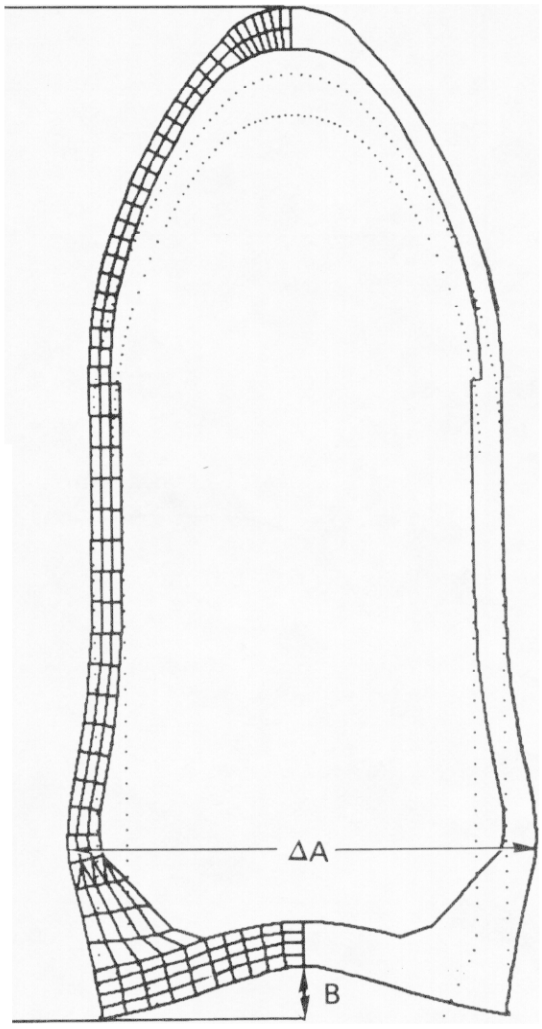

Analysis — Deformed Shape

Fig. 3. Preliminary Experimental/Analytical Correlation

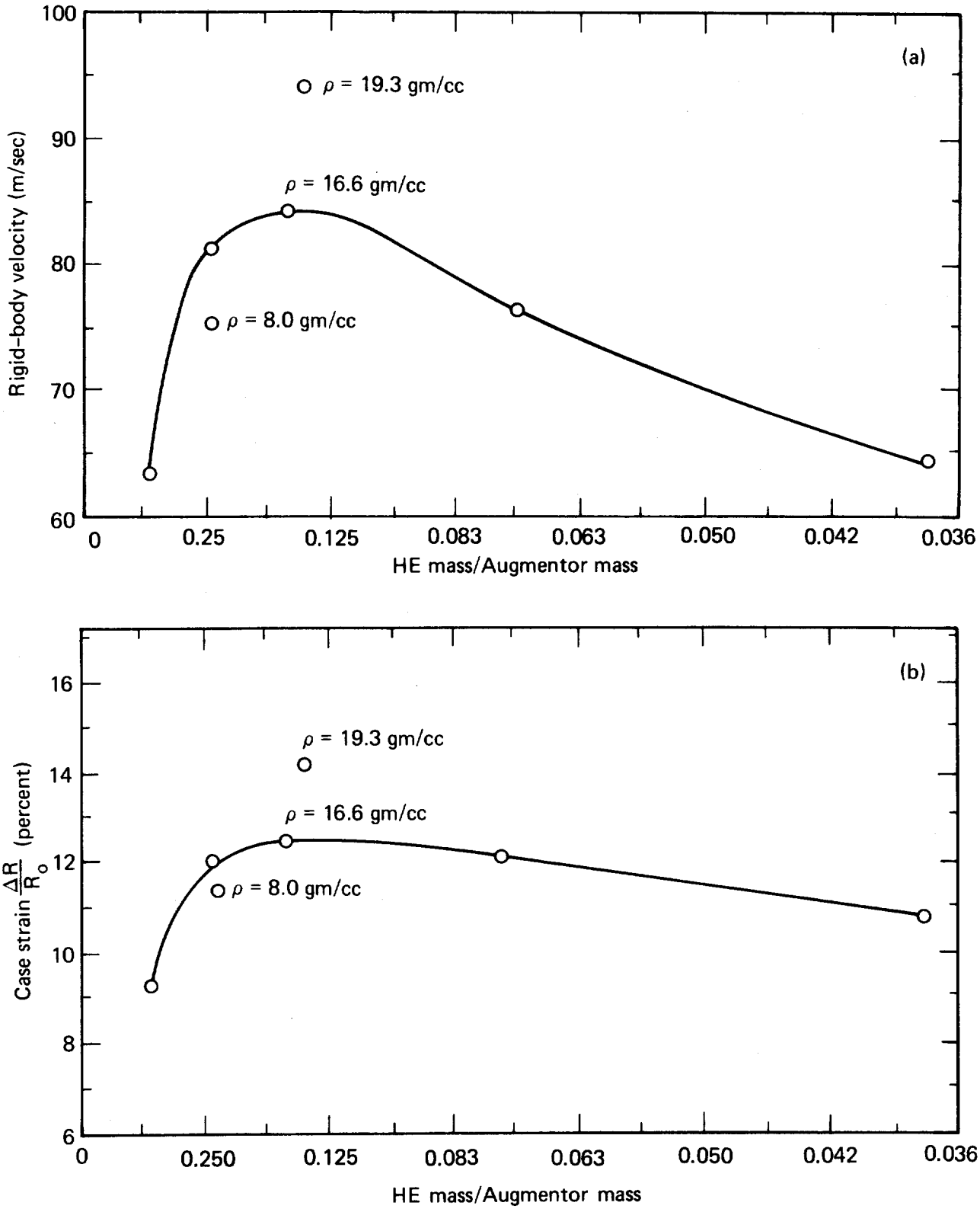

Fig. 4. Calculated Velocity and Strain Versus Charge to Mass Ratio

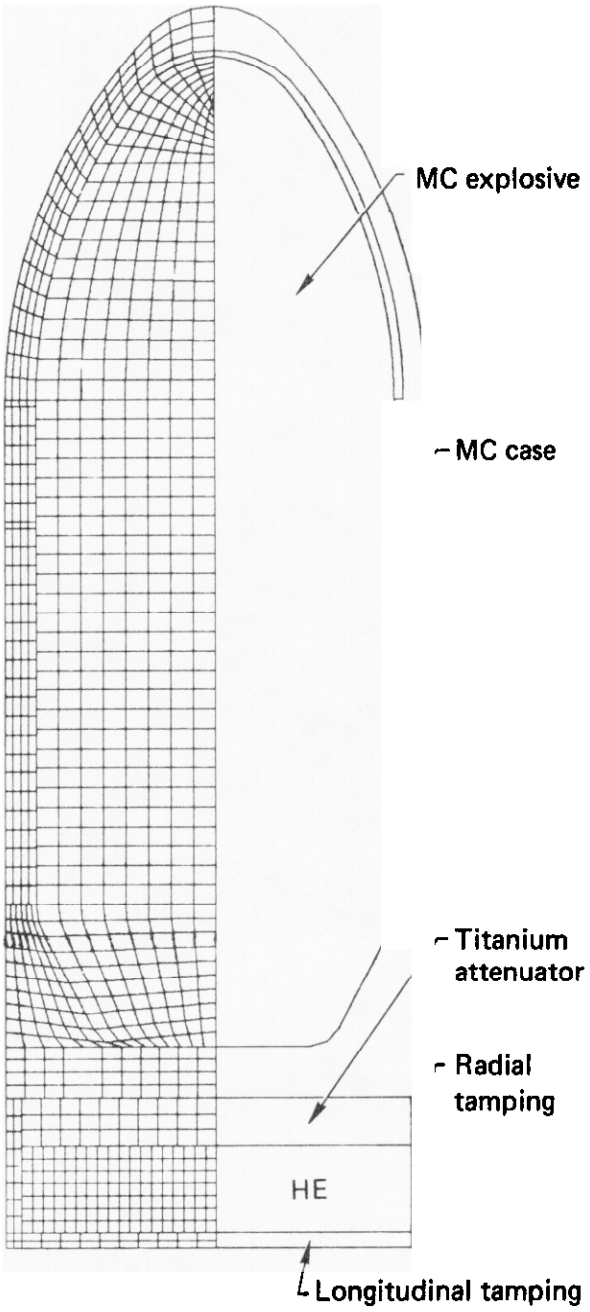

Fig. 5. Penetrator Assembly With Optimized Velocity Augmentor

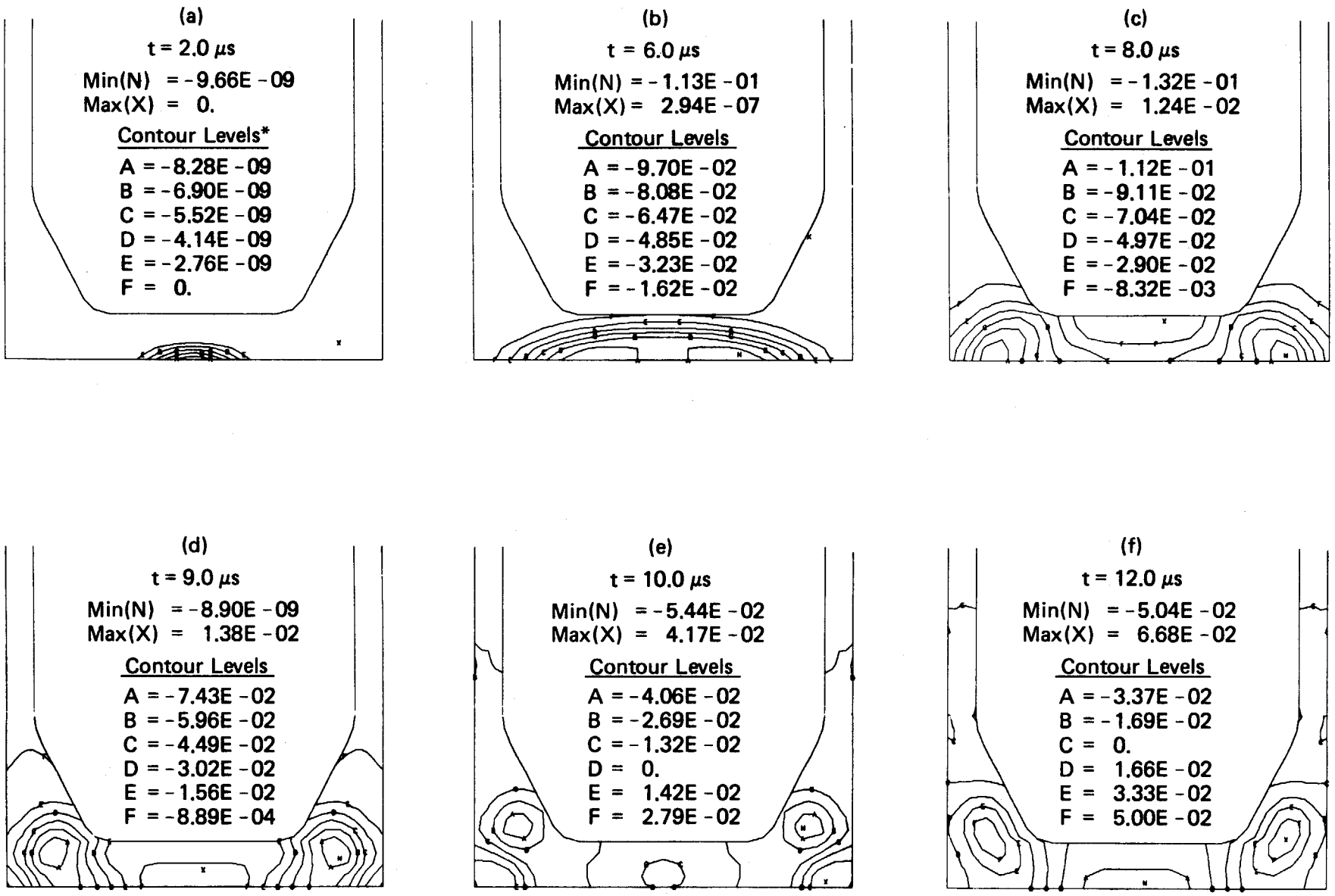

*Contour Levels in Mbar

Fig. 6. Shock Wave Propagation in Main Charge Case

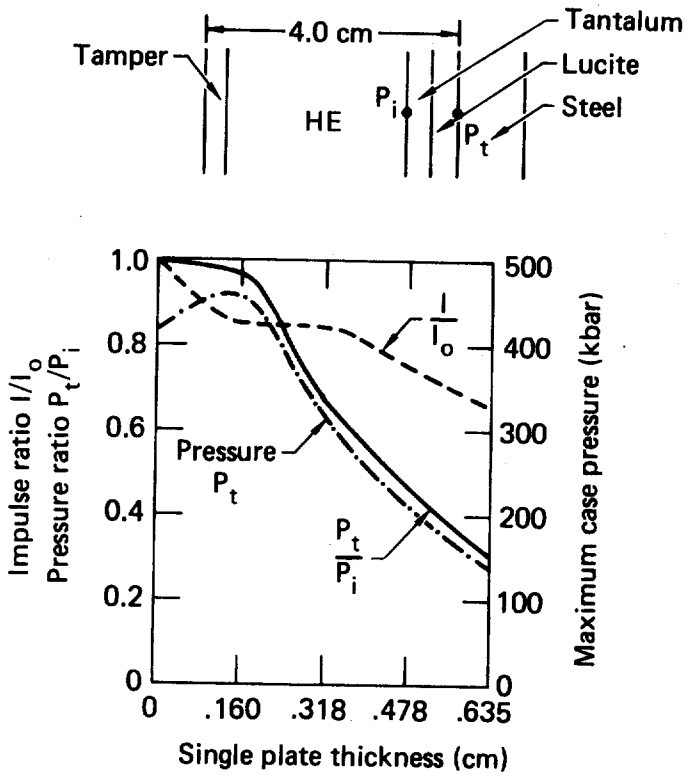

Fig. 7a. One-Dimensional Shock Attenuation Study

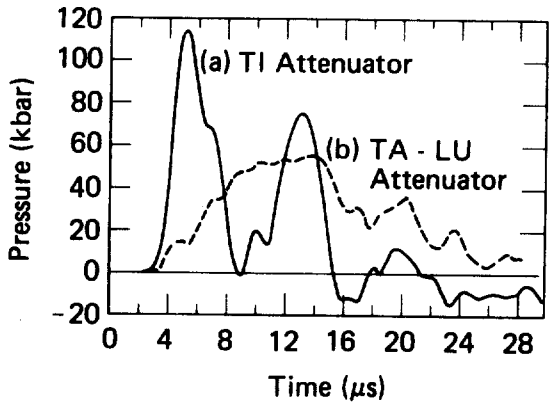

Fig. 7b. Calculated Two-Dimensional Base Pressure for Two Attenuators

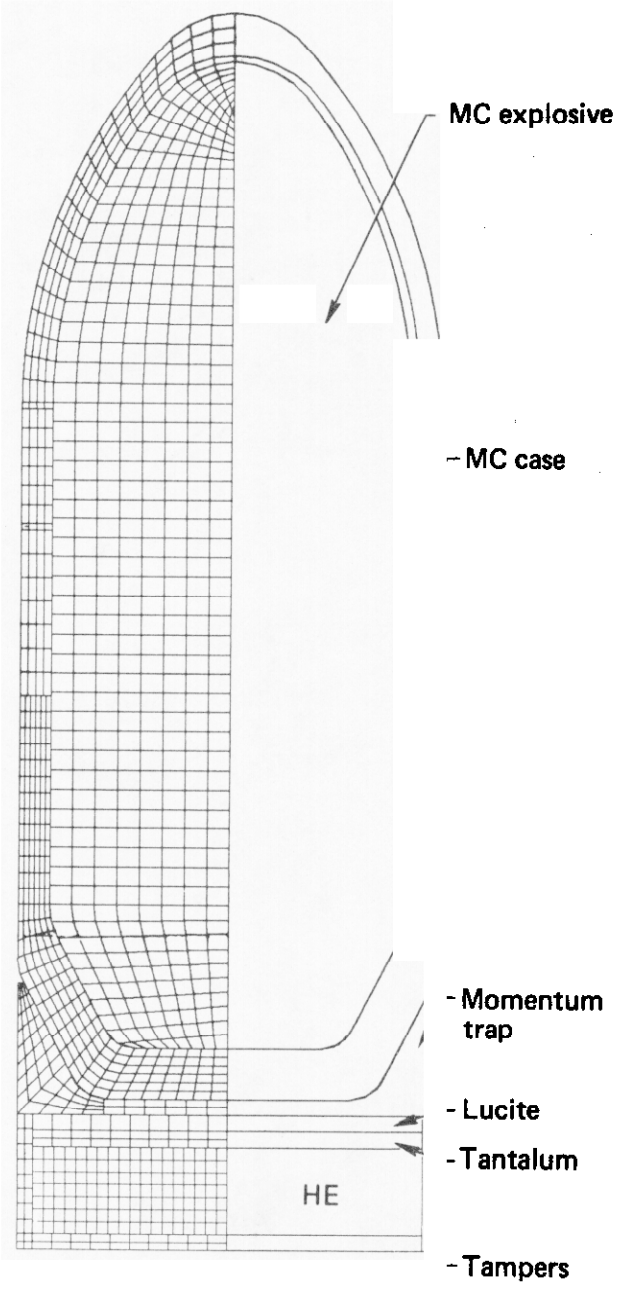

Fig. 8. Optimized Penetrator Assembly with Momentum Trap

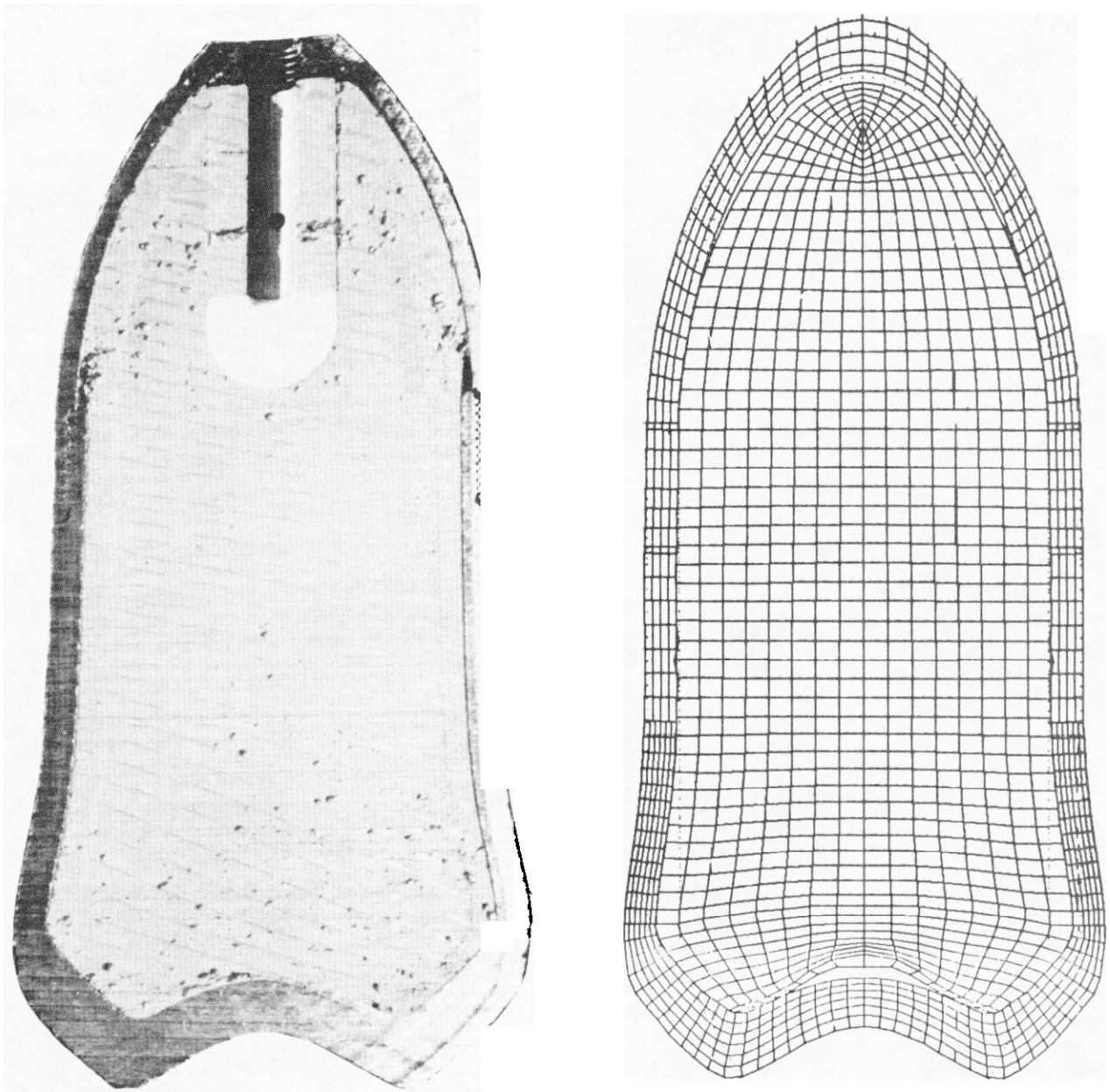

Fig. 9. Comparison of Final Experimental and Computed Deformed Geometries

REFERENCES

1. J. O. Hallquist, "DYNA2D -- An Explicit Finite Element and Finite Difference Code for Axisymmetric and Plane Strain Calculations," Lawrence Livermore Laboratory Report UCRL-52529.

2. D. J. Steinberg and M. W. Guinan, "A High-Strain-Rate Constitutive Model for Metals," Lawrence Livermore Laboratory Report UCRL-80465, 1978.

3. B. M. Dobratz, Ed., "Properties of Chemical Explosives and Explosive Simulants," Lawrence Livermore Laboratory Report UCRL-51319, Rev. 1, 1974.

4. J. O. Hallquist, "THOR -- A Post-Processor for Two-Dimensional Analysis Codes," Lawrence Livermore Laboraotory Report UCRL-52852.

5. M. J. Burger, "ZONE -- A Finite Element Mesh Generator," Lawrence Livermore Laboratory Report UCID-17139, Rev. 1.

6. Aerospace Structural Metals Handbook.

7. D. Breithaupt, Lawrence Livermore Laboratory, Private Communication (1979)

8. A. Weston, Lawrence Livermore Laboratory, Private Communication (1979)

9. J. P. Woodruff, "KOVEC User's Manual," Lawrence Livermore Laboratory Report UCID-17306, 1976.